Sensors and Materials, Vol. 13, No. 8 (2001) 461–475
MYU Tokyo

S & M 0462

Development of Microsensors for Measuring Electric Fields by Using Pockels Crystal

Tsuguhiro Takahashi

Central Research Institute of Electric Power Industry
2-6-1 Nagasaka, Yokosuka-shi, Kanagawa 240-0196, Japan

(Received April 2, 2001; accepted September 12, 2001)

Key words: electric field, measurement, Pockels, sensor, optical waveguide

A Pockels sensor for the direct measurement of electric fields has been studied. It is based on the utilization of an optical method and has many advantages as an electric field sensor. For example, it negligibly affects observed space. There is a demand to miniaturize sensors from the viewpoint of spatial resolution and the disturbance of the observed space, and the optical waveguide technique has been successfully introduced in the Pockels sensor. This paper presents the development of optical waveguide Pockels sensors. They utilize the Ti diffused $LiNbO_3$ optical waveguide whose width and depth are on the micrometer order. Their output signals show good linearity to applied AC and impulse electric fields. As one example of their application, electric fields with corona discharges are measured. The sensor shows signals according to discharge phenomena.

1. Introduction

In order to design and develop a power apparatus it is important to analyze electrical discharges, and the measurement of an electric field is extremely helpful in this regard. There are various methods for measuring the electric field.

The Pockels sensor is based on the utilization of an optical method and has the following advantages:[1] 1) It needs no metallic probe and negligibly affects the discharge space observed. 2) Information on the electric field is communicated in the form of light and thus the method is robust under electro-magnetic disturbances. 3) It has a broad frequency response in the range of DC to GHz.

The Pockels effect is a change in the refractive index of a crystal in proportion to an applied electric field.[2,3] A light beam in a Pockels crystal propagates with a refractive index depending on the electric field. Therefore, the electric field can be identified from the measurement of its phase shift.

There is a demand to miniaturize sensors from the viewpoint of spatial resolution. Some Pockels sensors using a bulk crystal whose dimensions are several mm to several cm have already been developed, but it seems that these dimensions are limited because of machining techniques. An optical waveguide technique has been introduced in the fabrication of Pockels sensors to achieve the spatial resolution of micrometers.

Previously, a z-cut x-propagation $LiNbO_3$ waveguide such as that which is conventionally used in optical communication devices has been utilized but it results in low sensitivity to the applied electric field and instability owing to thermal or mechanical disturbances.[4] A better configuration of the sensor has been proposed and realized.[5,6]

2. Measurement Principle

It is difficult to measure a phase shift of a light beam directly, so the interference between two kinds of light beams has been utilized in the Pockels sensor. In the case of the optical waveguide Pockels sensor in this study, a y-cut z-propagation (the light beam propagates along the z-axis) $LiNbO_3$ waveguide is used and two propagation modes, the TE mode and TM mode (shown in Fig. 1, strictly speaking, E^x_{pq} mode and E^y_{pq} mode, or TE-like mode and TM-like mode), detect the refractive index change through their interference.

These polarizations at the outlet of the waveguide can be given by

$$e_{TE} = A\sin\ \omega t \tag{1}$$

$$e_{TM} = A\sin(\omega t + \Gamma), \tag{2}$$

where A is amplitude, ω is angular frequency and Γ is the phase difference between e_{TE} and e_{TM}. They interfere with each other and the output light beam is detected with a photo diode. The output light power P_{out} is finally expressed by

$$P_{out} = \frac{1}{2}(1+\cos\Gamma)\cdot P_{in}, \tag{3}$$

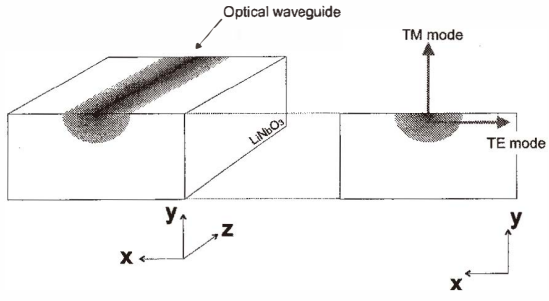

Fig. 1. Propagation modes in the waveguide.

where P_{in} is the input light power which is divided equally into the two modes. Equation (3) is illustrated in Fig. 2.

Due to the Pockels effect, the refractive indices in the waveguide for the two modes change in proportion to the applied electric field but they have different proportional constants. The phase difference Γ is expressed as a function of the applied field.

$$\Gamma = \Gamma_0 + \alpha E, \tag{4}$$

where Γ_0 is the phase difference in the case of no external electric field, α is a constant and E is the applied electric field along the y-axis, as shown in Fig. 1. The value of E can be determined by measuring P_{out}. Because the output signal changes around Γ_0, its value is one of the most important factors with respect to sensor sensitivity.

3. Transmission Light E-Field Sensor

A schematic diagram of a transmission light E-field sensor is shown in Fig. 3.[5,6] An electric field along the y-axis is measured using it. The light source is a semiconductor

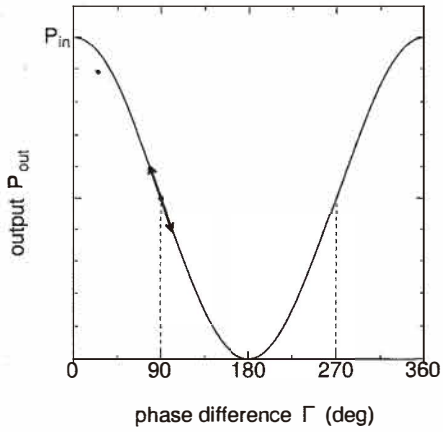

Fig. 2. Sensor output.

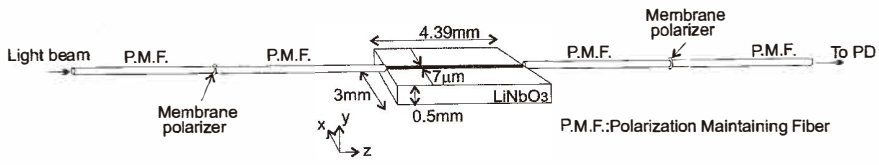

Fig. 3. Schematic diagram of transmission light E-field sensor.

laser whose wavelength is 1.31 μm. A single mode condition in the waveguide is satisfied for the laser. The light is led through a polarization maintaining fiber (P.M.F.) and its polarization is precisely adjusted to be linear using a thin membrane polarizer. A linearly polarized beam whose polarization direction is tilted at the angle of 45 degrees to the x-axis of the $LiNbO_3$ is led to a waveguide with a P.M.F. Then the TE and TM modes mentioned in the previous section are realized and propagate in the waveguide.

In this sensor the phase difference Γ_0 is adjusted to 90 degrees by cutting the waveguide to a length of 4.39 mm. The refractive index of the waveguide for the TE mode is slightly different from that for the TM mode in the case of no applied electric field. Using the difference in the refractive indices Δn, Γ_0 is given by

$$\Gamma_0 = \frac{2\pi}{\lambda} \Delta n \cdot L, \tag{5}$$

where λ is the wavelength of the light beam and L is the length of the waveguide. From some experimental data the value of L of 4.39 mm was chosen in order to adjust Γ_0 to 90 degrees.

At the outlet of the waveguide a polarization of the output light beam whose direction is tilted at the angle of 45 degrees to the x-axis is selectively transmitted by using a P.M.F. and a membrane polarizer.

Electrodes are attached to the waveguide in order to apply an electric field. Its outputs when AC and impulse voltages are applied are shown in Figs. 4 and 5. The rise time and halfwidth of the impulse voltage used are 0.2 μs and 8000 μs, respectively. The sensitivity to the applied AC electric field is shown in Fig. 6. and linearity between the output and the applied electric field is confirmed. The values of applied electric fields are computed by

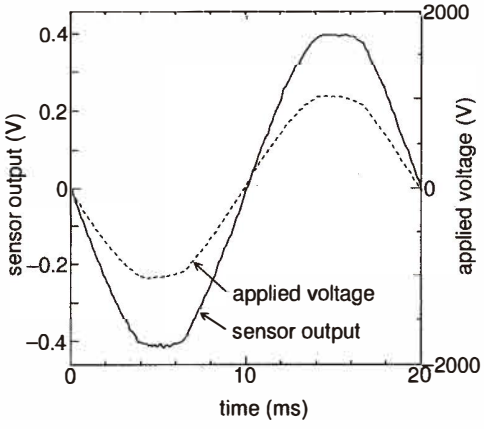

Fig. 4. Output signal of transmission light E-field sensor for applied AC voltage.

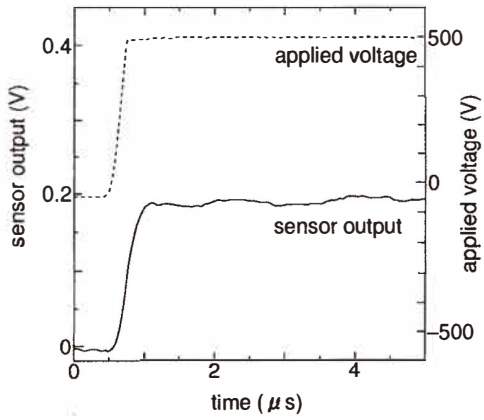

Fig. 5. Output signal of transmission light E-field sensor for applied impulse voltage.

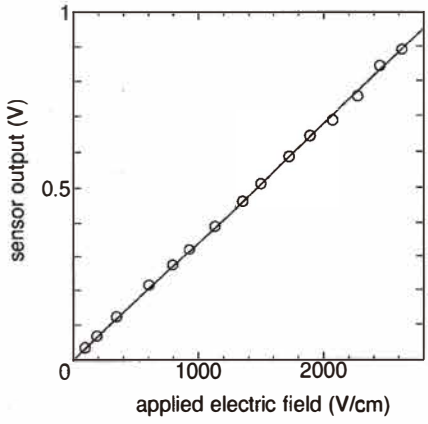

Fig. 6. Relationship between peak output value of transmission light E-field sensor and peak value of applied AC electric field.

using the charge simulation technique under experimental conditions. In this experiment, the minimum measured electric field is about 100 V/cm (internal value in the crystal). This value is determined by a signal to noise (S/N) ratio, so it depends on the stability of the light source and the photo detector circuit.

In Fig. 5, there is a slight delay. The rise time of the sensor output is about 300 ns for a step voltage with a rise time of about 200 ns. This must be caused not by the characteristics of the Pockels effect but by the time constant of the photo detector circuit.

In order to confirm this, an additional step response experiment with a high-frequency photo detector unit has been carried out. Its result is shown in Fig. 7. The photo detector unit has a frequency band of 1 GHz and relatively low sensitivity. The waveform of the applied voltage includes oscillating noise from the impulse generator, so after the rising phase it seems to be slightly different from that of the sensor output. However, there is no delay for rising phases of less than 10 ns. The frequency characteristic of the sensor sensitivity is shown in Fig. 8. The applied electric fields are controlled by a function generator and the output amplitude is normalized by the amplitude in the case of 50 Hz. A

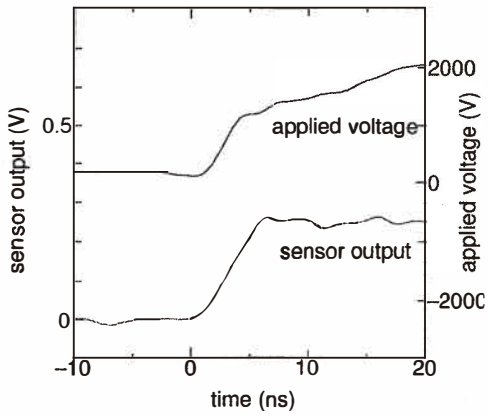

Fig. 7. Output signal of transmission light E-field sensor for applied impulse voltage with high-speed photo detector unit.

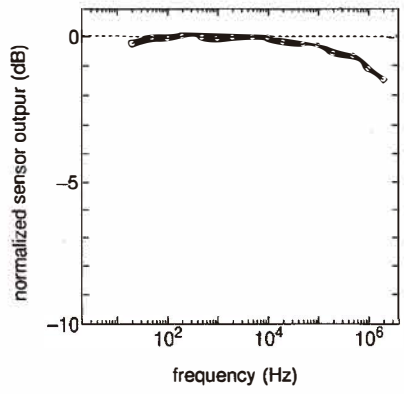

Fig. 8. Frequency characteristic of transmission light E-field sensor.

lowering of the sensor sensitivity in the high-frequency range is also caused by the frequency characteristic of the photo detector circuit. The time constant of the photo detector circuit must be determined by considering the frequency range of fields.

4 Improvement of E-Field Microsensor

Using the optical waveguide technique propagation light beams can be integrated in a narrow area. In order to confirm this advantage, Pockels sensors with shorter waveguides and two waveguides which are close to each other have been developed.

4.1 *Reflection light E-field sensors*

As mentioned in section 3, the value of Γ_0 is determined by the length of the waveguide L and the sensitivity of the sensor is decreased by reducing L. However, L also determines the spatial resolution and sensor head size, so it is desirable to utilize shorter waveguides in Pockels sensors for discharge measurement, and sensitivity should be secured by improving the S/N ratio (for example, by reducing the noise from the light source or the photo detector circuit). First, the value of L was adjusted to 1 mm and the configuration of the sensor is almost the same as that of the transmission light E-field sensor.[5,6] This sensor shows good linearity to applied electric fields, similar to the transmission light E-field sensor.

From the viewpoint of measurement convenience, a sensor having only one optical fiber on one side of the waveguide is more desirable than a sensor having a fiber on either side of the waveguide as mentioned above. Such a sensor has been developed using a dielectric mirror at the outlet face of the waveguide.[5]

A schematic diagram of this reflection light E-field sensor is shown in Fig. 9. A light beam is led to the waveguide through an optical coupler and a membrane polarizer. All fibers in this sensor system are P.M.F. The incident light beam has a linear polarization which is tilted at an angle of 45 degrees in the same way as the sensor mentioned in section 3. The light beam propagates in the waveguide and is reflected at the end face of the waveguide by a dielectric mirror. After propagating in the waveguide again, the reflected light beam passes out of the waveguide. The output light beam is divided into two beams by the optical coupler and one beam is led to a photo diode. An example of the reflection light E-field sensor is shown in Fig. 10.

All previously developed waveguide sensors need base boards made of glass (or other materials) to fix the waveguides and fibers. The sensor head size is determined not by the waveguide itself or the waveguide chip but by the base board. An extra small sensor that does not use a base board has been developed[7] and it is shown in Fig. 11. Its configuration is slightly different from that in Fig. 9. To improve the signal/noise ratio, a polarization splitter is utilized instead of a membrane polarizer, as shown in Fig. 12. It shows good linearity to applied electric fields, similar to the transmission light E-field sensor. This is the smallest class in the world of electric field sensors for free space. It is expected to be applied to point measurements in high-field areas such as the discharge space.

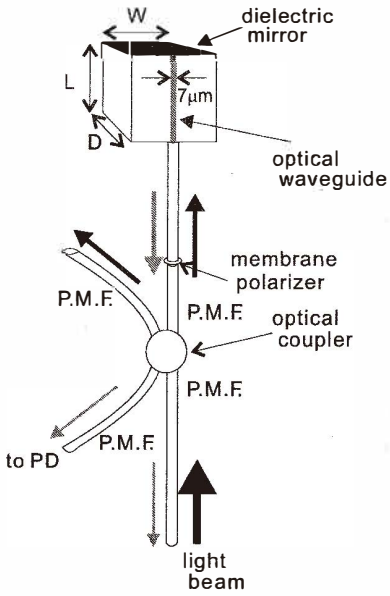

Fig. 9. Schematic diagram of reflection light E-field sensor.

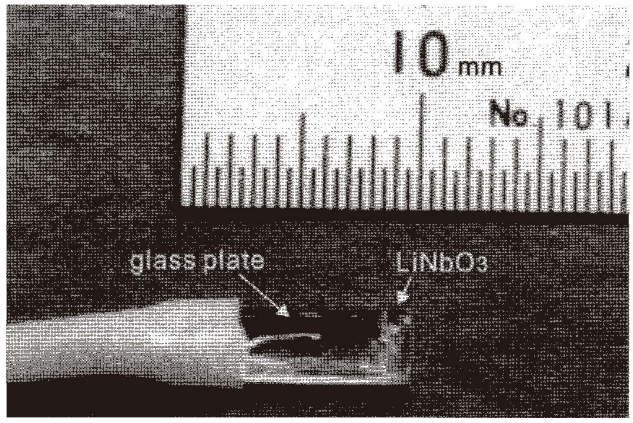

Fig. 10. Image of reflection light E-field sensor (L=1 mm, W=3 mm, D=0.5 mm in Fig .9).

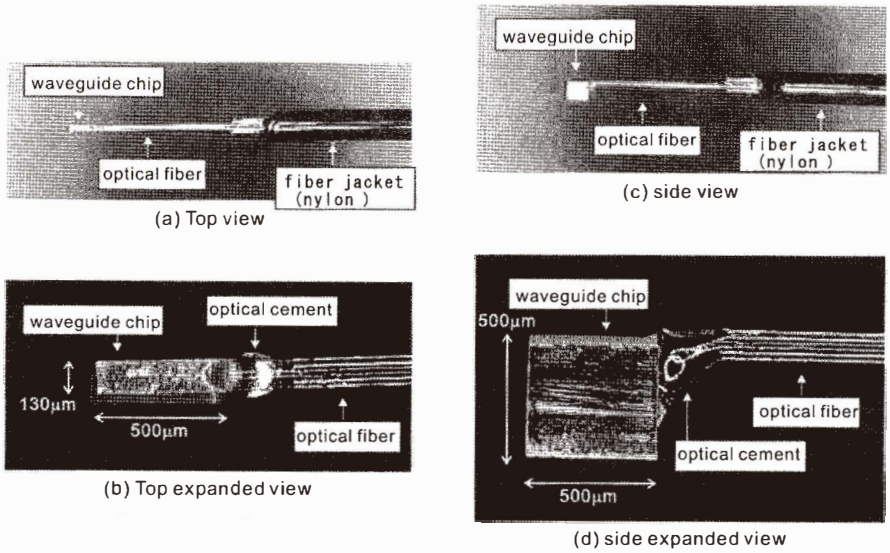

Fig. 11. Image of extra small sensor.

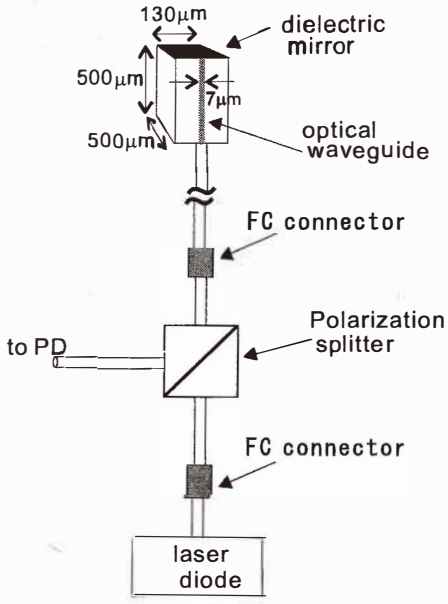

Fig. 12. Schematic diagram of extra small sensor.

4.2 *Double light beam close E-field sensor*

With the optical waveguide technique it is possible to fabricate many sensors in close proximity on one waveguide chip. Waveguides themselves can be formed at intervals of at least several hundred μm and each one can function as a sensor when connected with optical fibers. These sensors can make measurements at many points in a narrow region simultaneously.

Two sensors with an interval of 500 μm have been developed.[7] A schematic diagram and an image of these sensors are shown in Figs. 13 and 14, respectively. The configuration of each sensor is almost the same as that of the transmission light E-field sensor mentioned above. The sensitivity of these sensors is also simliar.

There are two waveguides whose widths are 7 μm and 6.8 μm on the $LiNbO_3$ chip with an interval of 500 μm. In these sensors the phase difference Γ_0 mentioned above is adjusted to about 90 degrees by cutting the waveguide to a length of 4.66 mm as in the transmission light E-field sensor. With these sensors, electric fields at two points with an interval of 500 μm can be measured simultaneously.

The AC electric fields of needle and plain electrodes have been measured with these

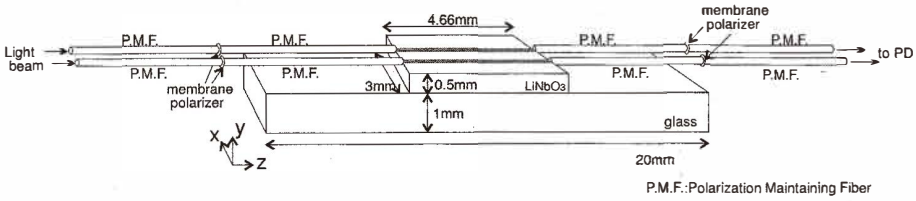

Fig. 13. Schematic diagram of double light beam close E-field sensor.

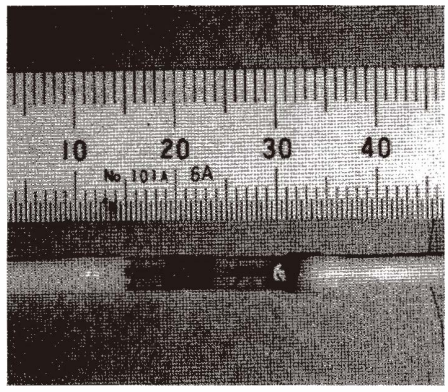

Fig. 14. Image of double light beam close E-field sensor.

sensors. The sensors are set on the plain electrode and the needle electrode is brought as close to the waveguide chip as possible without touching. The electric field distribution around the needle electrode is measured by moving it along the x direction as shown in Fig. 13. The result is shown in Fig. 15. These distributions measured with two sensors have the same form and there is 500 μm between their peak positions. Simultaneous two point measurement with an interval of 500 μm is confirmed by these results. By using more waveguides, applications to field distribution measurement are expected.

5 E-Field Measurement under Corona Discharge

As one example of measurement in discharge space, the surface electric fields of a high-voltage electrode from which corona discharge occurs are measured using the optical waveguide Pockels sensor.[8]

5.1 *Experimental setup*

The high-voltage electrode is cylindrical and the sensor is set up on the surface of the electrode. The waveguide and the fibers are fixed on a brass bed plate and installed in a short section of the cylindrical electrode as shown in Fig. 16. The cylinder has a narrow window, and the sensor is inserted there and fixed near the cylinder surface. There is a sensing window on the surface of the electrode.

The cylindrical electrode, whose length is 2 m and diameter is 38 mm, consists of the sensing section shown in Fig. 16, and two cylinders whose length is approximately 1 m. These cylinders are connected to either end of the sensing section. The electrode is fixed at a height of 1 m above a plane electrode earthed by two plastic rods as shown in Fig. 17. To the electrode, high AC voltages (~400 kV) are applied. The sensing window points downward. Optical fibers connected to the sensor are led out of both ends of the cylindrical

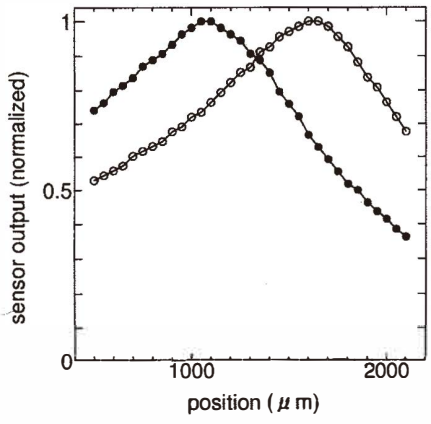

Fig. 15. Electric field distribution measured by double light beam close E-field sensor.

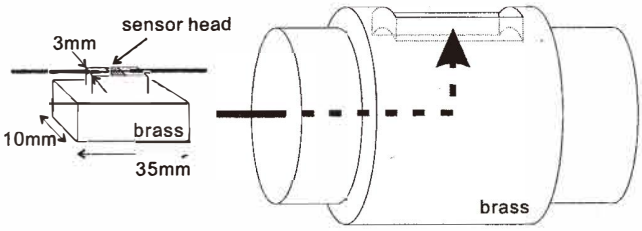

Fig. 16. Sensor setting.

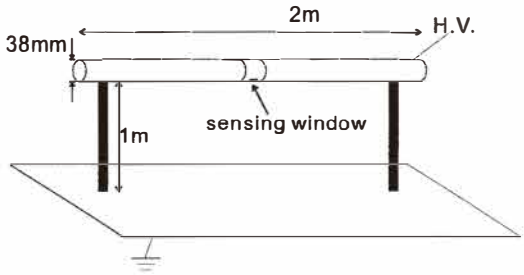

Fig. 17. Electrode system for measurement of corona discharge.

electrode. Their lengths are 10 m and 20 m, and a light source (a semiconductor laser whose wavelength is 1.31 μm) and a photo detector are set up in a safe area.

5.2 *Calibration*

In this case the measurement environment around the sensor is fixed, so calibration of the sensor output is carried out under the configuration shown in Fig. 17. With a certain applied voltage, a surface electric field can be calculated by a numerical method such as the charge simulation method. In this experiment the calibration factor is determined from sensor output and a calculation result with an AC voltage of 70 kV.

5.3 *Results*

Before corona discharge inception, the sensor output is proportional to an applied voltage. After corona discharge occurs, the waveform of the surface electric field is distorted and its peak value is restricted to about 30 kV/cm. This must be due to space charges around the electrode. The relationship between the peak values of applied voltages and surface electric fields is shown in Fig. 18. The surface electric fields of the cylindrical electrode were measured by a flux meter built into the cylinder.[9] The value of the restricted electric field differs because the diameter and gap length of the cylindrical electrode are different, but the same trend is observed. Because the flux meter in the cylindrical electrode must be rotated, its frequency characteristics are determined by the rotation speed. On the other hand, the Pockels sensor has a broad frequency response in the

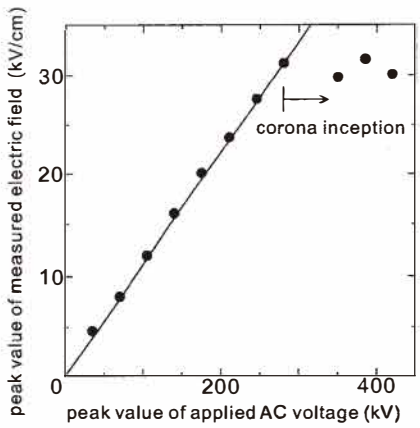

Fig. 18. Relationship between surface electric field and applied voltage.

range of DC to GHz. An example of sensor output during the corona discharge is shown in Fig. 19. The timing and strength of discharge can be observed in Fig. 19.

At more than 400 kV applied AC voltage there appears not only the corona discharge from the entire under electrode surface but also a partial discharge from the sensing window edge. An example is shown in Fig. 20. Figure 19 shows a relatively large partial discharge and charges attached to the surface of the waveguide chip. At a positive period of applied voltage a positive partial discharge occurs towards the earthed electrode and many electrons generated during this discharge ionization are attracted towards the cylindrical electrode. At the moment some of them attach to the surface of the waveguide chip, the sensor output suddenly increases to a large value. The reason there are two peaks is that there occurs a relaxation of the charges with a discharge between the sensing window edge and the waveguide chip surface.

During the next negative period, at first, because of negative charges on the waveguide chip, the sensor output remains positive. Then with almost the same phenomenon involving negative discharge and positive ions, the sensor output becomes negative. The mobility of positive ions is much smaller than that of electrons, and its change is slower. Because of this positive charge, at first during the positive period, the sensor output remains negative.

6. Conclusion

New optical waveguide Pockels sensors for measuring electric fields have been developed. These are based on a single waveguide on a y-cut $LiNbO_3$ crystal whose width is on the micrometer order (for example, 7 μm). They have the advantages of a simple configuration and a small size.

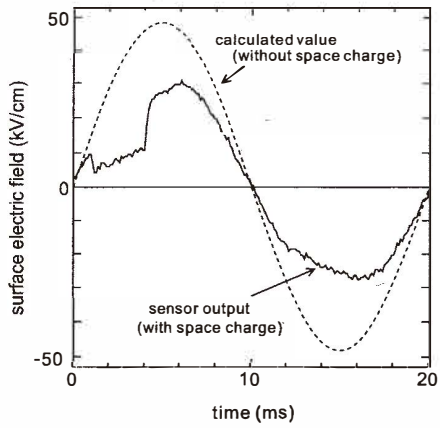

Fig. 19. Waveform of sensor output 1.

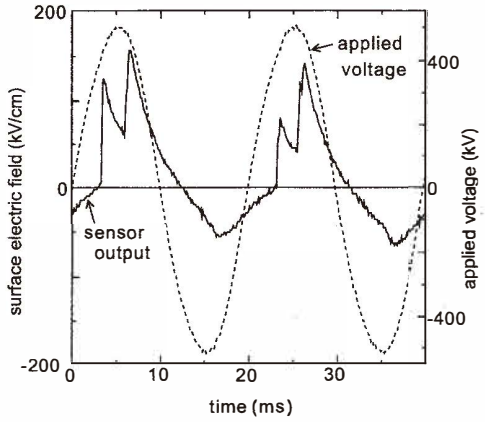

Fig. 20. Waveform of sensor output 2.

The transmission light E-field sensor has a waveguide of 4.39 mm in length together with an optical fiber at each end of the waveguide. In the small reflection light E-field sensors, only one fiber is connected to the 1 mm or 0.5 mm waveguide by means of a dielectric mirror at the outlet of the waveguide. Both AC and impulse electric fields are applied to all sensors and their response characteristics are examined. A good linearity between the output of the sensor and the applied field is confirmed for all sensors. Improvement of the minimum sensitivity is being investigated.

The double light beam close E-field sensor is fabricated on one waveguide chip with an interval of 500 μm. It can measure electric fields at two points in a narrow area simultaneously. The AC electric field distributions of needle and plain electrodes have been measured using this sensor.

As an example of sensor applications, corona discharges from a cylindrical electrode are measured using the optical waveguide Pockels sensor. They show output signals according to discharge space. As another application, measurement of surface discharges on PMMA plate is being carried out.[10]

References

1 K. Hidaka and Y. Murooka: Proc. of the 3rd Sensor Symposium (1983) p. 303.
2 A. Yariv and P. Yeh: Optical Waves in Crystals (Wiley, New York, 1984) Chap.7.
3 T. Tamir (ed.): Integrated Optics (Springer-Verlag, 1975) Chap. 2.
4 T. Takahashi, K. Hidaka, M. Chiba and T. Kouno: Proc. of 8th Int. Symp. on High Voltage Engineering, 54.09, Vol. 2 (1993) p. 407.
5 T. Takahashi, K. Hidaka and T. Kouno: Proc. of 9th Int. Symp. on High Voltage Engineering, Vol. 8 (1995) p. 8356.
6 T. Takahashi, K. Hidaka and T. Kouno: JJAP **35** (1996) 767.
7 T. Takahashi, T. Okamoto and K. Hidaka: Proc. of 10th Int. Symp. on High Voltage Engineering, Vol. 6 (1997) p. 89.
8 T. Takahashi: Proc. of 11th Int. Symp. on High Voltage Engineering, Vol. 2 (1999) p. 2.156.P6.
9 R. T. Waters: J. Phys. E **5** (1972) 475.
10 T. Takahashi: Proc. of 12th Int. Symp. on High Voltage Engineering, Vol. 2, No.4-97 (2001) p. 578.